Appl. Phys. B 90, 445–449 (2008)
DOI: 10.1007/s00340-007-2909-y

Applied Physics B
Lasers and Optics

T. OMATSU[1,✉]
A. MINASSIAN[2]
M.J. DAMZEN[2]

Passive Q-switching of a diode-side-pumped Nd-doped mixed gadolinium yttrium vanadate bounce laser

[1] Graduate School of Advanced Integration Science, Chiba University, 1-33, Yayoi-cho, Inage-ku, Chiba 263-8522, Japan
[2] Department of Physics, Imperial College London, Prince Consort Road, London SW7 2BW, UK

Received: 9 October 2007 / Revised version: 5 November 2007
Published online: 22 January 2008 • © Springer-Verlag 2008

ABSTRACT High power passive Q-switching was achieved with a pulse width of 18–32 ns by using a diode-side-pumped Nd:$Gd_{0.6}Y_{0.4}VO_4$ bounce amplifier. An average output power of >8 W was obtained at a pump power of 39 W. The peak power of the Q-switched output was adjusted within 1.9–5.2 kW by changing the Nd concentration. The mixed vanadates showed significantly higher Q-switching performances in comparison with pure Nd:$GdVO_4$.

PACS 42.55.Xi; 42.60.Gd; 42.60.Da

1 Introduction

Passively Q-switched solid-state lasers employing a saturable absorber (SA) such as Cr^{4+}:YAG have been intensely investigated because no additional electronic elements are required and they provide robust and inexpensive alternatives to actively Q-switched systems. Passively Q-switched lasers, mainly formed in an end-pumped microchip laser geometry, mostly have the drawback of lower output power due to the residual absorption of the saturable absorbers producing output powers of ~ 4 W [1–3].

A diode-side-pumped bounce amplifier configuration based on neodymium-doped vanadate slabs including Nd:YVO_4 and Nd:$GdVO_4$, in which extremely high inversion density is produced below the pump face of the amplifier, is a promising candidate for producing high power outputs at ultra-high efficiency and high beam quality [4–6]. The bounce amplifier geometry will allow an easier power scaling of the passively Q-switched laser systems in comparison with the conventional end-pumping geometry, even with the residual absorption of the saturable absorbers.

However, very large emission cross sections of Nd:YVO_4 and Nd:$GdVO_4$ frequently prevent stable passive Q-switching, and yield pre-lasing and pulse broadening in the Q-switching operation. Villafana et al. demonstrated a passively Q-switched Nd:YVO_4 bounce laser using a LiF:F^2 saturable absorber, demonstrating ~ 2 W stable Q-switched output with minimum pulse width of ~ 10 ns [7]. However, the peak power of the Q-switched pulses was limited to ~ 0.5 kW.

Use of *c*-cut Nd-doped vanadates (or *a*-axis-pumped vanadates) is one solution to produce successfully high peak power Q-switching pulses [8]. However, the use of *c*-cut vanadates showing low absorption ($\sim 11\,\mathrm{cm}^{-1}$) for the pump diode wavelength forms a deeper pumped region (~ 3 mm), which would impact total performance of the bounce laser system.

Mixed vanadate technology, in which, for example, a fraction of Gd ions in the $GdVO_4$ are replaced by Y ions, is capable of customizing the fluorescence spectrum, thereby allowing production of adjustable laser parameters such as stimulated emission cross section and fluorescence lifetime [9–12]. Recently, we demonstrated an actively Q-switched Nd-doped mixed gadolinium yttrium vanadate (Nd:$Gd_xY_{1-x}VO_4$) laser with custom-made pulse repetition frequency (PRF) range of 100–650 kHz and peak power range of 1–3 kW [13].

In this paper, we extend our mixed vanadate bounce laser work to develop a high average power passively Q-switched laser. We demonstrate stable Q-switching operation of a diode-side-pumped mixed gadolinium yttrium vanadate (Nd:$Gd_xY_{1-x}VO_4$) bounce laser at a pulse repetition frequency range of up to 150 kHz and a pulse duration in the range of 18–32 ns. The average power in Q-switched operation was 5.1–8.2 W at a pump power of 40 W. The corresponding peak power of 1.9–5.2 kW was achieved.

2 Experiments

2.1 *Continuous-wave operation*

Figure 1 shows the schematic diagram of the bounce amplifier setup. The amplifiers used for the experiment were two *a*-cut, 2 mm × 5 mm × 20 mm slabs, i.e. a 1 at. % Nd-doped Gd-rich mixed vanadate Nd:$Gd_{0.6}Y_{0.4}VO_4$ slab and a 1.5 at. % Nd-doped $Gd_{0.6}Y_{0.4}VO_4$ slab (Hortek Crystal Co., Ltd). The amplifiers, having two end faces antireflection coated for 1 μm, were wedged to the normal of the pump face to prevent self-lasing within the crystal. A continuous-wave (cw) 808-nm diode array output was delivered by a 12.7 mm cylindrical lens (CL_D) to be a line focus with dimensions of ~ 0.2 mm × 15 mm on the pump face of the amplifiers.

✉ Fax: +81-43-290-3490, E-mail: omatsu@faculty.chiba-u.jp

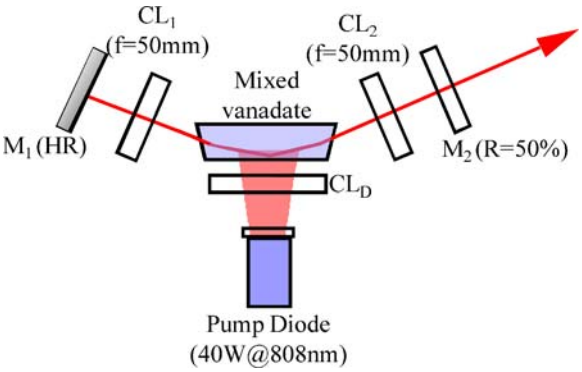

FIGURE 1 Experimental setup for cw operation

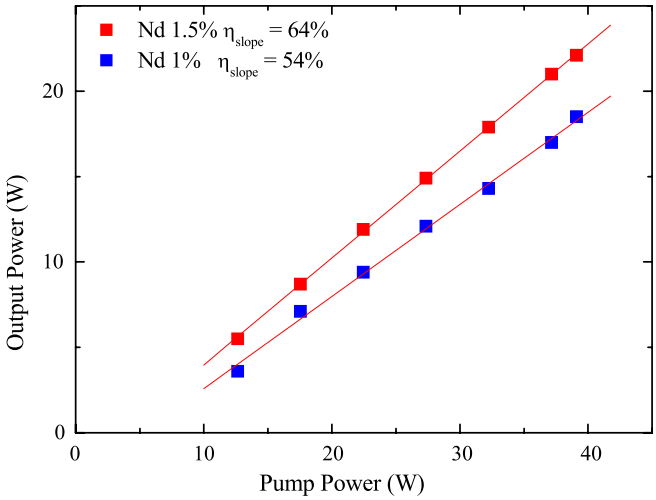

FIGURE 2 Experimental plots of the cw output power as a function of pump power

The laser cavity was the same as that used in our previous publications, and it was composed of a highly reflective flat mirror M for 1064 nm, a partially reflective flat output coupler OC also for 1064 nm and two cylindrical lenses, CL_1 and CL_2 ($f = 50$ mm), in the vertical direction for spatially matching the laser mode to the ellipsoidal gain region. The internal incidence angle of the laser mode with respect to the pump face normal was $\sim 80°$.

We measured the cw output power from the mixed vanadate lasers using various output couplers. The optimum reflectivity of the output coupler for both the mixed vanadate crystals used was $\sim 50\%$. The 1.5 at. % $Nd:Gd_{0.6}Y_{0.4}VO_4$ showed slightly lower lasing threshold and higher slope efficiency in comparison with those of the 1 at. % $Nd:Gd_{0.6}Y_{0.4}VO_4$. Maximum output power of 22 W was obtained at the pump power of 39 W (Fig. 2), corresponding to a slope efficiency of 64%. The higher Nd doping produced a relatively shallower pumped region, yielding higher laser gain and resulting in highly efficient laser oscillation with the slope efficiency of $> 60\%$.

2.2 *Passively Q-switched operation*

A 4.4-mm-long, 0.3%-doped Cr^{4+}:YAG crystal with initial optical density of 0.42 was used as saturable absorber for passive Q-switching. The criterion to achieve stable

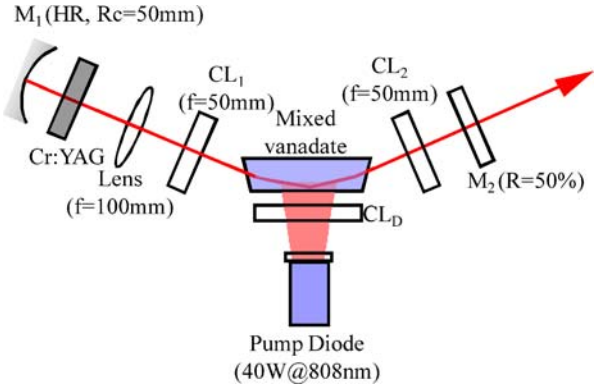

FIGURE 3 Experimental setup for passively Q-switched operation

Q-switching is given by the following expression [14]:

$$\frac{\ln\left(1/T_0^2\right)}{\ln\left(1/T_0^2\right)+\ln(1/R)+L}\,\frac{\sigma_a}{\sigma_e}\,\frac{A_e}{A_a} > \frac{1}{1-\beta}\,, \tag{1}$$

where T_0 (~ 0.45) is the transmission of the unsaturated saturable absorber, R is the reflectivity of the output coupler, L (0.02) is the internal loss of the cavity, σ_a (3×10^{-18} cm^2) is the ground-state absorption cross section of the saturable absorber, σ_e (7×10^{-18} cm^2) is the stimulated emission cross section of the gain medium, β (0.25) is the ratio of the excited-state absorption cross section to the ground-state absorption cross section and A_e/A_a is the ratio of the laser mode areas in the gain medium and in the saturable absorber. By substituting the physical parameters into (1), stable Q-switching requires the value $A_e/A_a > 0.8$. To satisfy the criterion and achieve stable passive Q-switching, the cavity configuration was modified as shown in Fig. 3. The Cr:YAG crystal was located near a confocal point of the focusing lens ($f = 100$ mm) and a spherical mirror ($R = 50$ mm). The reflectivity of the output coupler was 10%.

Above the pump power (~ 20 W) required to achieve threshold, the laser started to operate in Q-switched mode, and its output exhibited a smooth temporal profile without mode beating as shown in Fig. 4a. In the case of the 1 at. % Nd-doped Gd-rich mixed vanadate $Nd:Gd_{0.6}Y_{0.4}VO_4$ slab amplifier, the threshold of Q-switched operation was ~ 18 W and a slope efficiency of 20% was obtained. The pulse repetition frequency was 22 kHz near threshold, increasing to 52 kHz at the maximum pump level (39 W). The pulse width was typically ~ 20 ns at all pump levels, resulting in peak powers in the range of 3.7–5.2 kW.

In the case of the 1.5 at. % Nd-doped mixed vanadate slab amplifier, a slope efficiency of 40% was achieved and the maximum output power reached 8.2 W. As shown in Fig. 4b, the output exhibited a slightly broader pulse width (~ 30 ns) in the PRF region of 45–153 kHz, resulting in the peak power being limited to ~ 1.9 kW. The higher laser gain and the reduced fluorescence lifetime observed in the highly doped mixed vanadate prevent larger energy storage.

To compare the performances of the mixed vanadates with conventional 1.1 at. % $Nd:GdVO_4$, we also measured the Q-switched output power from a $Nd:GdVO_4$ laser (Fig. 4c).

Figure 5 summarizes the Q-switched performance of three vanadate lasers including two mixed vanadates and $GdVO_4$.

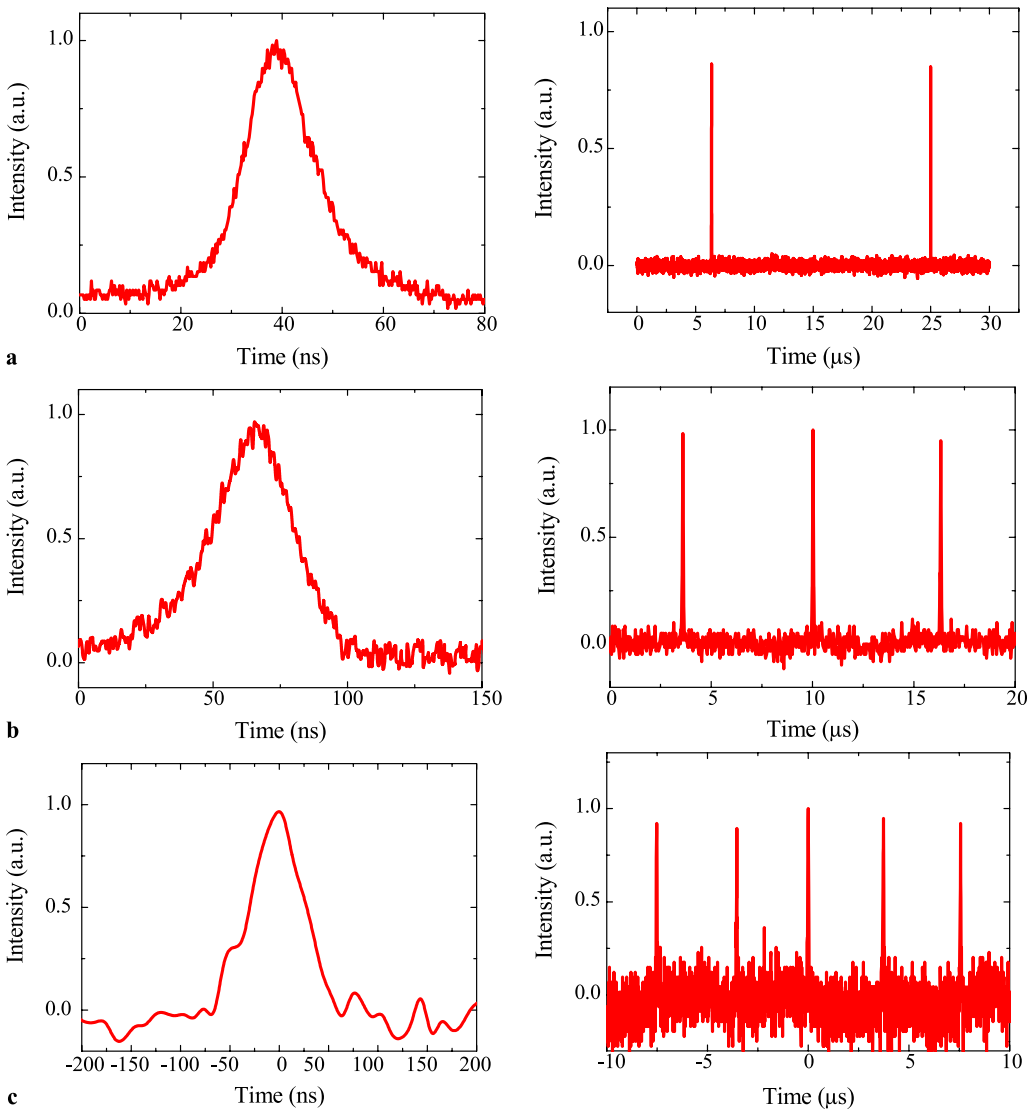

FIGURE 4 Temporal evolutions of the Q-switched pulse in (**a**) 1 at. % Nd:$Gd_{0.6}Y_{0.4}VO_4$, (**b**) 1.5 at. % Nd:$Gd_{0.6}Y_{0.4}VO_4$ and (**c**) Nd:$GdVO_4$

The peak power of the output was limited to ∼ 0.6 kW, while the average output power was similar to that of 1.5 at. % Nd-doped mixed vanadate. The pulse width of the output was typically ∼ 50 ns. At the maximum pump level, the PRF increased to 252 kHz, which is comparable to the maximum PRF of stable Q-switching expected from the recovery time of saturable absorption (∼ 3 μs). These results show that too strong gain in the Nd:$GdVO_4$ amplifier prevented production of intense Q-switched pulses with high peak power.

The output exhibited a mixed-mode profile as shown in Fig. 6. The corresponding M^2 factor of the output along the horizontal axis was ∼ 2.5, while the M^2 factor along the vertical was 1.2, and it was relatively small in comparison with that (∼ 5) of the cw output previously reported by us. This means that the saturable absorber produced a limiting aperture for the laser to operate at lower-order modes.

3 Numerical simulations

The rate equations for passive Q-switching with the Cr:YAG crystal can be written as follows [15]:

$$\frac{\mathrm{d}n}{\mathrm{d}t} = \frac{\eta_{\mathrm{pump}} P_{\mathrm{pump}}}{V}\left(\frac{\lambda_{\mathrm{p}}}{hc}\right) - c\sigma_{\mathrm{e}} n\varphi - c\sigma_{\mathrm{esa}} n\varphi - \frac{n}{\tau_{\mathrm{f}}}, \tag{2}$$

$$\frac{\mathrm{d}\varphi}{\mathrm{d}t} = c\sigma_{\mathrm{e}} n\varphi \frac{l_{\mathrm{g}}}{l} - c\sigma_{\mathrm{a}} n_{\mathrm{a}}\varphi \frac{l_{\mathrm{a}}}{l}\frac{A_{\mathrm{e}}}{A_{\mathrm{a}}} - \frac{\varphi}{\tau_{\mathrm{c}}} + \frac{n}{\tau_{\mathrm{f}}}\Omega, \tag{3}$$

$$\frac{\mathrm{d}n_{\mathrm{a}}}{\mathrm{d}t} = c\sigma_{\mathrm{a}}(N_0 - n)\varphi \frac{A_{\mathrm{e}}}{A_{\mathrm{a}}} - \frac{n_{\mathrm{a}}}{\tau_{\mathrm{a}}}, \tag{4}$$

$$\frac{1}{\tau_{\mathrm{c}}} = \frac{2l}{c}\left(\ln\left(\frac{1}{R}\right) + L_{\mathrm{i}}\right), \tag{5}$$

where n is the inversion population density, φ is the photon density, η_{pump} is the pump quantum efficiency, P_{pump} is the pump diode power, V is the volume of the pumped region, hc/λ_{p} is the photon energy of the pump diode, c is the velocity of light, σ_{esa} is the excited-state absorption cross section of the Cr:YAG crystal, τ_{f} is the fluorescence lifetime of the upper level, τ_{a} is the decay time of the excited level in the Cr:YAG crystal, l_{g} is the length of the pumped region, l_{a} is the length of the saturable absorber, l is the cavity length, Ω is the factor accounting for the fraction of spontaneous photons contributing to the lasing, n_{a} is the population density of the excited state in the Cr:YAG crystal and N_0 is the total

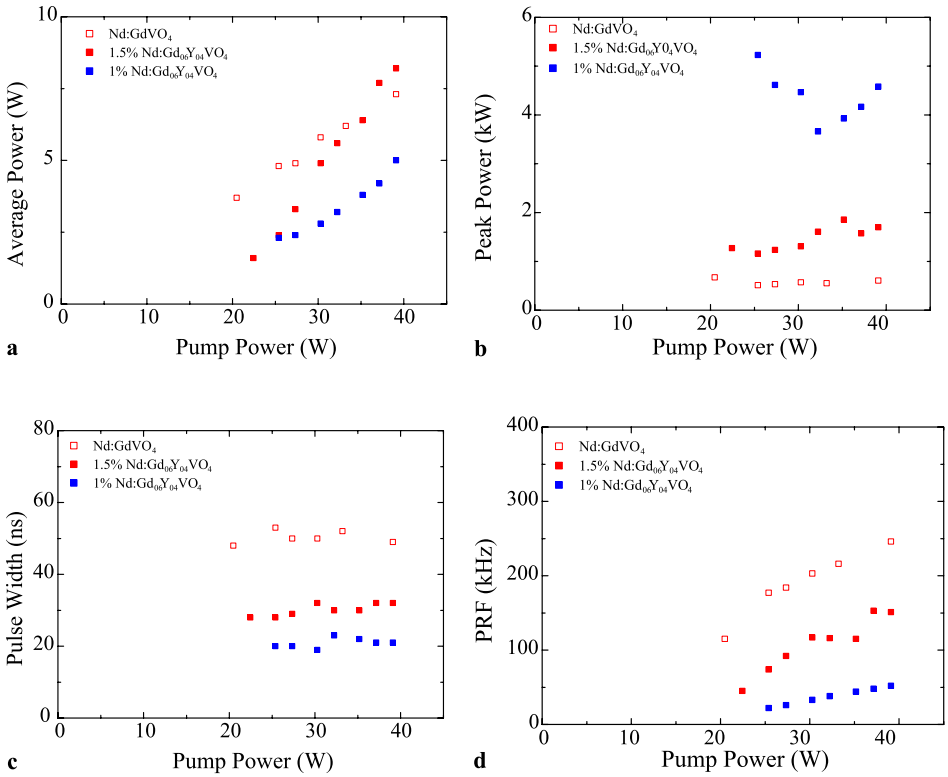

FIGURE 5 Experimental data in Q-switching operation. (**a**) Average power, (**b**) peak power, (**c**) pulse width and (**d**) pulse repetition frequency as a function of pump power

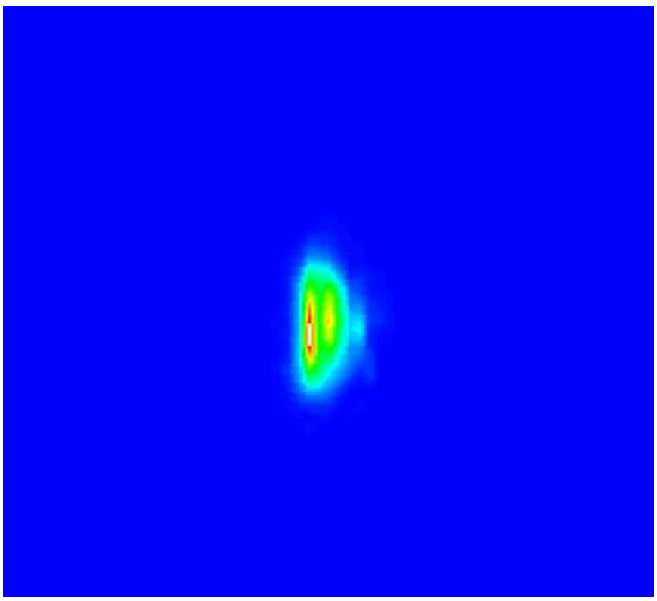

FIGURE 6 Spatial form of the Q-switched output

number of the Cr ions, respectively. By using the values given in Table 1, we numerically simulated the theoretical temporal evolution of Q-switched pulses. The ratio A_e/A_a of the laser mode areas was difficult to estimate accurately, and it was optimized within the range of 1.3–2. Three curves (red and blue solid curves, and red broken curve) in Fig. 7 show the simulated plots as a function of the pump power. The simulated PRF in the mixed vanadates increases as the pump power increases, and there is good agreement between simulations and experiments. The simulated pulse width of the Q-switched output in the mixed vanadates is also consistent with the experimental one, though there is a slight mismatch of the absolute value between simulation and experiment.

In the case of $GdVO_4$, the simulated pulse width of the Q-switched output increases gradually above the pump power of 30 W, while the experimental one is constant within the whole pump range. The discrepancy between simulation and experiment in Nd:$GdVO_4$ will be due to uncertainties of the physical parameters.

4 Conclusion

We have successfully demonstrated passive Q-switching of mixed gadolinium yttrium vanadate Nd:$Gd_xY_{1-x}VO_4$ slab lasers with a bounce amplifier geometry, for the first time. By changing the Nd doping, we can adjust the peak power (1.9–5.2 kW) and pulse repetition frequency regions (22–145 kHz) of the stable Q-switching operation. We have also compared the Q-switching performance of the mixed vanadate lasers with that of a conventional Nd:$GdVO_4$ laser. The mixed vanadate slabs are capable of producing higher peak power Q-switched pulses in comparison with the conventional vanadate crystals.

At even higher pumping, severe thermal effects of the saturable absorber will significantly impact the performance of the stable Q-switching operation. For further power scalability, careful cavity design, that would include thermal issues of the Cr:YAG crystal, will be necessary.

We can also extend the system to optimize the product of peak and average powers for nonlinear frequency conversion by varying the initial absorption of the Cr:YAG crystal.

ACKNOWLEDGEMENTS The authors acknowledge support from the Joint Research Project of the Japan Society for the Promotion of

TABLE 1 Physical parameters for numerical simulation

	Parameter, unit	Value
n_{pump}	Pump quantum efficiency	1
P_{pump}	Maximum pump power, W	40
V	Laser volume, cm^3	0.003
λ_p	Wavelength of pump diode, cm	0.8×10^{-4}
σ_e	Stimulated emission cross section, cm^2	7×10^{-19} ($Nd:Gd_{0.6}Y_{0.4}VO_4$) 12.6×10^{-19} ($Nd:GdVO_4$)
τ_f	Spontaneous fluorescence lifetime, μs	100 (1 at. % $Nd:Gd_{0.6}Y_{0.4}VO_4$) 85 (1.5 at. % $Nd:Gd_{0.6}Y_{0.4}VO_4$) 100 ($Nd:GdVO_4$)
σ_a	Absorption cross section, cm^2	30×10^{-19}
σ_{esa}	Absorption cross section of excited state, cm^2	7.5×10^{-19}
τ_a	Recovery time of saturable absorption, μs	3
l	Cavity length, cm	40
l_e	Active length, cm	2
l_a	Absorption length, cm	4.4
Ω	Spontaneous emission factor	1.0×10^{-5}
R	Reflectivity of output coupler	0.1
L_i	Internal dissipative optical losses	0.02
A_e/A_a	Ratio of the laser mode areas in the amplifier and absorber	1.9 (1 at. % $Nd:Gd_{0.6}Y_{0.4}VO_4$) 1.4 (1.5 at. % $Nd:Gd_{0.6}Y_{0.4}VO_4$)

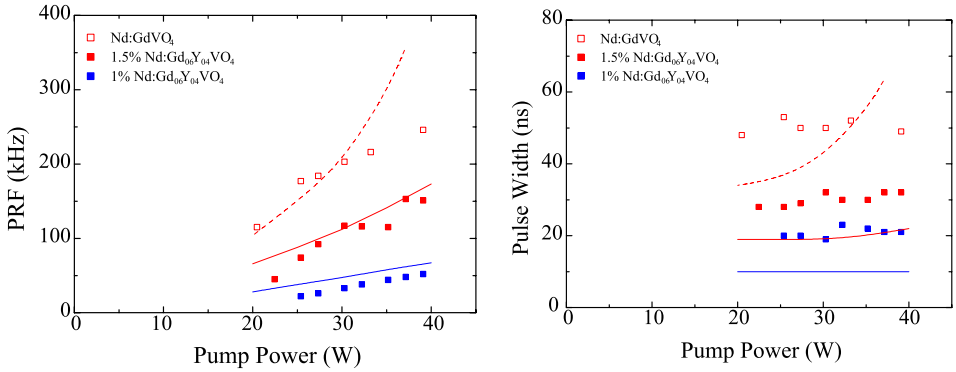

FIGURE 7 PRF and pulse width of Q-switched output from mixed vanadate slab lasers. *Red* and *blue squares* show experimental results in 1.5 at. % $Nd:Gd_{0.6}Y_{0.4}VO_4$ and 1 at. % $Nd:Gd_{0.6}Y_{0.4}VO_4$ lasers, respectively. *Red* and *blue solid curves* show the simulated plots. Results for pure $Nd:GdVO_4$ are shown for comparison

Science, and the Engineering Physical Science Research Council (UK) under Grant No. GR/T08555/01.

REFERENCES

1 C. Li, J. Song, D. Shen, N.S. Kim, J. Lu, K. Ueda, Appl. Phys. B **70**, 471 (2000)
2 C. Du, J. Liu, Z. Wang, G. Xu, X. Xu, K. Fu, X. Meng, Z. Shao, Opt. Laser Technol. **34**, 699 (2002)
3 A. Agnesi, S. Dell'acqua, Appl. Phys. B **76**, 351 (2003)
4 J.E. Bernard, A.J. Alcock, Opt. Lett. **19**, 1861 (1994)
5 A. Minassian, B. Thompson, M.J. Damzen, Appl. Phys. B **76**, 341 (2003)
6 B. Thompson, A. Minassian, M.J. Damzen, 42 W $Nd:GdVO_4$ bounce laser oscillator, in *Technical Digest of the Conference on Lasers and Electro-Optics (CLEO 2004)*, San Francisco, CA (2004), paper CThJJ2
7 E.R. Villafana, A.V. Kir'yanov, A. Minassian, M.J. Damzen, Laser Phys. **15**, 1 (2005)
8 S. Forget, F. Druon, F. Balembois, P. Georges, N. Landru, J.-P. Fe've, J. Lin, Z. Weng, Opt. Commun. **259**, 816 (2006)
9 J. Liu, X. Meng, Z. Shao, M. Jiang, B. Ozygus, A. Ding, H. Weber, Appl. Phys. Lett. **83**, 1289 (2003)
10 H. Zhang, J. Wang, C. Wang, L. Zhu, X. Hu, X. Meng, M. Jiang, Y.T. Chow, Opt. Mater. **23**, 449 (2003)
11 J. Liu, Z. Wang, X. Meng, Z. Shao, B. Ozygus, A. Ding, H. Weber, Opt. Lett. **28**, 2330 (2003)
12 Y.F. Chen, M.L. Ku, L.Y. Tsai, Y.C. Chen, Opt. Lett. **29**, 2279 (2004)
13 T. Omatsu, M. Okida, A. Minassian, M.J. Damzen, Opt. Express **14**, 2727 (2006)
14 J. Liu, B. Ozygus, S. Yang, J. Erhard, U. Seelig, A. Ding, H. Weber, X. Meng, L. Zhu, L. Qin, C. Du, X. Xu, Z. Shao, J. Opt. Soc. Am. B **20**, 652 (2003)
15 W. Chen, Y. Inagawa, T. Omatsu, M. Tateda, N. Takeuchi, Y. Usuki, Opt. Commun. **194**, 401 (2001)